X-622-74-124
PREPRINT

NASA TM X- 70672

POLAR SYMMETRIC FLOW OF A VISCOUS COMPRESSIBLE ATMOSPHERE; AN APPLICATION TO MARS

JOSEPH A. PIRRAGLIA

MAY 1974

GSFC

GODDARD SPACE FLIGHT CENTER
GREENBELT, MARYLAND

For information concerning availability
of this document contact:

Technical Information Division, Code 250
Goddard Space Flight Center
Greenbelt, Maryland 20771

(Telephone 301-982-4488)

POLAR SYMMETRIC FLOW OF A VISCOUS COMPRESSIBLE ATMOSPHERE; AN APPLICATION TO MARS

Joseph A. Pirraglia

May 1974

The Laboratory for Planetary Atmospheres

Goddard Space Flight Center

Greenbelt, Maryland

ABSTRACT

The atmosphere is assumed to be driven by a polar symmetric temperature field and the equations of motion in pressure ratio coordinates are linearized by considering the zero order in terms of a thermal Rossby number $R\Delta T/(2a\Omega)^2$, where ΔT is a measure of the latitudinal temperature gradient. When the eddy viscosity is greater than 10^6 cm^2/sec the boundary layer extends far up into the atmosphere making the geostrophic approximation invalid for the bulk of the atmosphere. The surface pressure gradient exhibits a latitudinal dependence opposite that of the depth averaged temperature. The magnitude of the gradient is dependent upon the depth of the boundary layer, which depends upon the eddy viscosity, the boundary conditions imposed at the surface, and upon the temperature lapse rate. Using a temperature model for Mars based on Mariner 9 infrared spectral data with a 30% increase in the depth averaged temperature from the winter pole to the subsolar point, the following results were obtained for the increase in surface pressure from the subsolar point to the winter pole as a function of eddy viscosity and with no-slip conditions imposed at the surface:

eddy viscosity (cm^2/sec)	percent change in surface pressure
10^6	9
10^7	17
10^8	37

The meridional cellular flow rate is also correlated with the eddy viscosity, causing a complete overturning of the atmosphere in tens of days for an eddy

viscosity of 10^8 cm^2/sec and in hundreds of days for 10^6 cm^2/sec. The implication of this overturning in the dust storm observed during the early part of the Mariner 9 mission is discussed briefly.

CONTENTS

1. Introduction

Zonal geostrophic motion of the atmosphere is often used as the basic flow upon which more complex flow regimes are constructed. Its simplicity and, in many cases, apparent approximation of observational data makes it an attractive assumption. However, as a basic state a more adequate description may sometimes be desirable. As will be shown, if the atmosphere is vertically unstable such that a large eddy viscosity is probable, the layer within which the geostrophic approximation is valid is confined to the upper regions of the atmosphere thereby eliding a large mass of the atmosphere from the assumed basic state. Differential heating in the latitudinal direction of a rotating inviscid planetary atmosphere causes zonal geostrophic motion with the result that there is no latitudinal redistribution of mass. However, when viscosity or damping are introduced geostrophy is disrupted and there is a resultant meridional flow with a latitudinal pressure gradient that is no longer arbitrary as in geostrophic flow which adjusts itself to any imposed pressure field. The linearized dynamic equations with the viscous terms retained predict Hadley cell circulation in addition to the zonal motion, the geometry and flow associated with the cells being dependent upon the temperature gradient and the magnitude of the viscous terms.

Polar symmetric flow as a limiting case of tidal theory with damping was considered for Mars by Pirraglia and Conrath (1974). Linear damping proportional to the velocity was assumed and the shearing stress terms were ignored which precluded the possibility of satisfying the horizontal velocity boundary conditions at the surface. The latitudinal surface pressure gradient turns out to be independent of the magnitude of the damping coefficient and dependent upon

only the gradient of the vertically mass averaged temperature. On the other hand, the wind field, in particular the meridional component, is strongly dependent upon the damping coefficient. The use of a linear damping term gives a poor description of the upper atmosphere where it does not predict predominantly geostrophic flow.

Differentially heated fluids in rotating annuli have been treated by Robinson (1959) and Barcilon and Pedlosky (1967a, 1967b) among others. In these papers the Boussinesq approximation is made and while Robinson discusses a homogeneous fluid, Barcilon and Pedlosky discuss a stratified fluid. Robinson expands the equations in terms of a thermal Rossby number and uses boundary layer analysis where the Ekman number is the small parameter. Barcilon and Pedlosky assume that the Rossby number is less than the Ekman number and expand in 1/2 powers of the Ekman number with the dynamic variables being sums of interior fields and boundary-layer corrections, which is equivalent to the boundary-layer analysis. These latter papers indicate the striking effect of stratification on rotating fluid flow as compared to the homogeneous case. (The book by Greenspan (1968) gives a fairly extensive treatment of rotating fluids.)

In this paper we shall consider a formal solution to the Navier-Stokes equations, with eddy viscosity in place of molecular viscosity, for polar symmetric flow in which the density is determined from the perfect gas law and the atmosphere is in approximate hydrostatic equilibrium with vertical velocities due to horizontal divergence. The problem is not approached as a boundary layer problem since a substantial part of the total mass of the atmosphere could be strongly influenced by the boundary conditions if the viscosity is large. Spiegel and Veronis (1959) point out that a basic assumption of the Boussinesq

approximation is that the density variation through the depth of the atmosphere is small compared to the average density. Since this is not true for the full depth of the atmosphere, in addition to the fact that to the zero order we will consider an essentially homogeneous condition, the Boussinesq approximation is not used. The linearized zero order solution is the first iteration of a set of nonlinear integrodifferential equations whose resultant flow is a combination of Hadley cell circulation, an Ekman-like velocity profile and approximate geostrophic flow at high altitudes.

Specific results are presented in which the temperature field is based upon temperature data obtained by the infrared spectroscopy experiment on Mariner 9 and the eddy viscosity is assumed to be constant with altitude. The results of this application show the dependence of latitudinal pressure gradient upon the temperature field, the magnitude of the eddy viscosity and the boundary conditions. Also shown is the correlation of the thickness of the boundary layer with the eddy viscosity, independent of the boundary conditions, and the meridional flow rates associated with the eddy viscosity and boundary conditions. From the results one can determine the validity of the geostrophic approximation under differing conditions and the difficulty due to boundary condition uncertainties, in predicting the flow within the outer boundary layer in even a relatively simple model. The meridional flow rates lead to speculations concerning the dust storm observed during the early part of the Mariner 9 mission.

2. Dynamic Equations

The problem to be considered is the time invariant symmetric state of a rotating shallow viscous atmosphere with an imposed polar symmetric temperature field. Effects of curvature are neglected and the atmosphere is assumed

to be very close to being in vertical hydrostatic equilibrium and to obey the perfect gas law. To simplify the analysis the equations will be expressed in σ-coordinates (Phillips, 1957) where the vertical coordinate σ is the ratio of the atmospheric pressure at altitudes within a column to the pressure at the base of the column.

The following symbols are defined:

$\underline{v}$ horizontal velocity vector on a constant σ-plane,

$\dot{\sigma}$ vertical velocity,

π surface pressure,

T temperature,

Φ geopotential,

T_e radiative equilibrium temperature,

τ radiative relaxation time,

R gas constant for atmosphere,

c_p specific heat of atmosphere at constant pressure,

κ R/c_p

θ colatitude,

ϕ longitude,

σ vertical coordinate,

H mean pressure scale height,

K_M momentum eddy diffusivity,

K_H heat eddy diffusivity,

$\underline{k}$ unit vertical vector,

Ω rotational speed of planet,

a radius of planet,

ξ cosine of the colatitude,

∇ horizontal gradient operator.

The symbols $\underline{v}, \dot{\sigma}$, T, π, Φ and ∇ with asterisks are dimensioned variables and without asterisks are dimensionless variables.

If the eddy diffusivity terms are of the form

$$\frac{1}{\rho} \frac{\partial}{\partial z} \rho K_M \frac{\partial \underline{v}^*}{\partial z} \tag{1}$$

$$\frac{1}{\rho} \frac{\partial}{\partial z} \rho K_H \left(\frac{\partial T^*}{\partial z} + \frac{g}{c_p} \right), \tag{2}$$

then using the mean pressure scale height H in place of an altitude dependent scale height (1) and (2) can be written in σ-coordinates as

$$\frac{\partial}{\partial \sigma} \left(\frac{\sigma^2}{H^2} K_M \frac{\partial \underline{v}^*}{\partial \sigma} \right) \tag{3}$$

$$\frac{\partial}{\partial \sigma} \left[\frac{\sigma^2}{H^2} K_H \left(\frac{\partial T^*}{\partial \sigma} - \kappa \frac{T^*}{\sigma} \right) \right] . \tag{4}$$

If H were the true scale height the expressions (3) and (4) would be exactly equivalent to (1) and (2) but are reasonable approximations if the mean scale height is used.

Using (3) and (4), the time invariant equations describing the flow are

$$2\xi\Omega\underline{k} \times \underline{v}^* + \underline{v}^* \cdot \nabla \underline{v}^* + \dot{\sigma}^* \frac{\partial \underline{v}^*}{\partial \sigma} + \nabla \Phi^* + \frac{RT^*}{\pi^*} \nabla^* \pi^* - \frac{\partial}{\partial \sigma} \left(\frac{\sigma^2}{H^2} K_M \frac{\partial \underline{v}^*}{\partial \sigma} \right) \tag{5}$$

$$- K_M \nabla^{*2} \underline{v}^* = 0$$

$$\Phi^* = -R\int_1^{\sigma}\frac{T^*}{s}\,ds + \Phi_1^* \tag{6}$$

$$\dot{\sigma}^* = -\frac{1}{\pi}\int_1^{\sigma}\nabla^*\cdot(\pi^*\underline{v}^*)\,ds \tag{7}$$

$$Q = c_p\underline{v}^*\cdot\nabla^*T^* + c_p\dot{\sigma}^*\frac{\partial T^*}{\partial\sigma} - \frac{RT^*}{\sigma\pi^*}(\pi^*\dot{\sigma}^* + \sigma\dot{\pi}^*) - c_p\frac{\partial}{\partial\sigma}\left[\frac{\sigma^2}{H^2}K_H\left(\frac{\partial T^*}{\partial\sigma} - \kappa\frac{T^*}{\sigma}\right)\right] \tag{8}$$

$$- c_pK_H\nabla^{*2}T^* + c_p\frac{T^* - T_e^*}{\tau^*},$$

where in (6) and (7) s is an integration variable. The vertical velocity $\dot{\sigma}^*$ is equal to zero at the planet's surface $\sigma = 1$ and at the top of the atmosphere $\sigma = \sigma_0$. The boundary conditions on the horizontal velocity will be expressed as a linear combination of the velocity and its vertical shear equal to $\underline{v}_a^*$ at $\sigma = \sigma_0$ and $\underline{v}_b^*$ at $\sigma = 1$. The energy equation (8) is assumed to be radiatively damped as expressed in the last term on the right hand side with the radiative equilibrium temperature specified everywhere and the dynamically induced temperature specified on the boundaries.

Using the average surface pressure π_0 to define the dimensionless pressure $\pi = \pi^*/\pi_0$, and using the maximum latitudinal temperature difference ΔT to define the speed $U = R\Delta T/(2a\Omega)$, the dimensionless variables $\underline{v} = \underline{v}^*/U$, $\dot{\sigma} = \dot{\sigma}^*(a/U)$ and $T = T^*/\Delta T$ are defined. The dimensionless gradient operator is defined by $\nabla = a\nabla^*$. Using the dimensionless quantities in equations (5) through (8) and defining a thermal Rossby number $\beta = R\Delta T/(2a\Omega)^2$ and an Ekman number $\epsilon = K_M/(2\Omega H^2)$, the dimensionless dynamic equations are

$$\xi \underline{k} \times \underline{v} + \beta \left(\underline{v} \cdot \nabla \underline{v} + \dot{\sigma} \frac{\partial \underline{v}}{\partial \sigma} \right) + \nabla \Phi + T \nabla \ln \pi - \epsilon \frac{\partial}{\partial \sigma} \left(\sigma^2 \frac{\partial \underline{v}}{\partial \sigma} \right) - \frac{H^2}{a^2} \epsilon \nabla^2 \underline{v} = 0 \qquad (9)$$

$$\dot{\sigma} = -\frac{1}{\pi} \int_1^{\sigma} \nabla \cdot (\pi \underline{v}) \, ds \qquad (10)$$

$$\Phi = -\int_1^{\sigma} \frac{T}{s} ds. \qquad (11)$$

With the Prandtl number $P = K_M / K_H$ and the dimensionless radiative damping time constant $\tau = 2 \Omega \tau^*$ the dimensionless heat equation is

$$\frac{P}{2\Omega c_p \Delta T} Q = \beta P \left[\underline{v} \cdot \nabla T + \dot{\sigma} \frac{\partial T}{\partial \sigma} - \kappa T \left(\frac{\dot{\sigma}}{\sigma} + \frac{\dot{\pi}}{\pi} \right) \right] + \epsilon \frac{\partial}{\partial \sigma} \left[\sigma^2 \left(\frac{\partial T}{\partial \sigma} - \kappa \frac{T}{\sigma} \right) \right] + \frac{H^2}{a^2} \nabla^2 T + P \frac{T - T_e}{\tau}. \qquad (12)$$

The temperature field is assumed to be the sum of an imposed temperature field $T_0 = T_e$ independent of the large scale dynamics and the temperature βT_β which is due to the dynamics. Then with $T = T_0 + \beta T_\beta$ (12) can be expressed as

$$\epsilon \frac{\partial}{\partial \sigma} \left[\sigma^2 \left(\frac{\partial T_\beta}{\partial \sigma} - \kappa \frac{T}{\sigma} \beta \right) \right] + \epsilon \frac{H^2}{a^2} \nabla^2 T_\beta - P \frac{T_\beta}{\tau} = -P \left[\underline{v} \cdot \nabla T + \dot{\sigma} \frac{\partial T}{\partial \sigma} - \kappa T \left(\frac{\dot{\sigma}}{\sigma} + \underline{v} \cdot \nabla \ln \pi \right) \right]. \qquad (13)$$

The square of the ratio of the scale height to the planet radius being a very small number, the horizontal diffusion terms in (9) and (13) can be neglected. With this approximation and using a Green's function involving integration in σ only, the set of equations (9), (10), (11) and (13) can be expressed as a set of

integrodifferential equations which can be solved iteratively. Here we shall be concerned with the velocity only to the zero order in β and with the temperature field to the first order. In the zero order approximation T_0 is the temperature field driving the system and the dynamically induced temperature T_β is obtained from (13) using the zero order terms in the right hand side of the equation.

With $T = T_0$ and using the perfect gas law, equations (10), (11) and the zero order momentum equation,

$$\xi \underline{k} \times \underline{v} - \epsilon \frac{\partial}{\partial \sigma} \left(\sigma^2 \frac{\partial \underline{v}}{\partial \sigma} \right) + \nabla \Phi + T \nabla \ln \pi = 0, \tag{14}$$

form a complete set, sufficient to solve for the horizontal and vertical velocities and the surface pressure. Equation (14) represents the balance between the pressure, coriolis force and viscous effects. In regions in which ξ or ϵ are large compared to β the nonlinear terms of (9) can be neglected. Such regions would be those sufficiently far from the equator or in the boundary layer where there is appreciable wind shear. When ϵ is of the order of unity[1] equation (14) is a good approximation over all regions except at very high altitudes in the equatorial plane. For smaller values of ϵ the linearized equations are a good approximation in all regions except practically the full depth of the equatorial zone.

Although the fluid is compressible, the zero order flow is essentially the same as homogeneous flow since a moving parcel of fluid assumes the ambient

[1] For example if Mars with a 10 km scale height had an eddy diffusivity of 10^8 cm^2/sec ϵ would be of the order of .5 and β approximately .05.

temperature imposed by the zero order temperature field. The motion would be nonisentropic if it were assumed that heat is supplied or extracted so as to maintain the zero order temperature. However, if it is assumed that the only heating is that necessary to maintain the zero order temperature without the flow, as stated above, and if the dynamic contribution T_β is small the flow is still essentially homogeneous but adiabatic. When T_β is appreciable compared to T_0 its effect on the flow must be considered and the phenomena associated with stratification will become apparent. In our formulation such effects would be determined iteratively.

3. Method of Solution

Expressing the velocity $\underline{v}$ in complex form $v = v_\phi + iv_\theta$, where v_θ is the meridional velocity and v_ϕ is the zonal velocity, and using the symmetry of the applied temperature field, equation (14) in complex form is

$$-i\epsilon \frac{\partial}{\partial\sigma}\left(\sigma^2 \frac{\partial v}{\partial\sigma}\right) + \xi v = \frac{\partial\Phi}{\partial\theta} + T\frac{\partial}{\partial\theta} \ln\pi \equiv F \tag{15}$$

The boundary conditions on $v(\sigma)$ are

$$\text{(a)} \qquad v(\sigma_0)\cos\alpha_a + v'(\sigma_0)\sin\alpha_a = v_a$$

$$\text{(b)} \qquad v(1)\cos\alpha_b + v'(1)\sin\alpha_b = v_b \tag{16}$$

where the prime indicates the derivitive with respect to σ. The choice of α_a, α_b, v_a and v_b allows the boundary conditions to be specified in terms of the velocity, the velocity shear or a linear combination of the velocity and shear. The Green's function solution of (15) is discussed in Appendix I.

Letting G represent integration over the homogeneous Green's function and G_a and G_b the boundary contributions, the solution to (15) is

$$v = G(F) + G_b v_b + G_a v_a. \tag{17}$$

Assuming that any surface velocity will be proportional to the surface pressure gradient we can write $v_b = S_b \partial/\partial\theta \ln \pi$. Similarly, assuming that conditions at the top of the atmosphere will be dependent upon the surface pressure and the geopotential we define $v_a = S_a \partial/\partial\theta \ln\pi + v_{a0}$. The terms S_a, S_b and v_{a0} will be defined below. From the definition of F in (15) and the preceeding discussion,

$$v = G\left(\frac{\partial\Phi}{\partial\theta} + T\frac{\partial}{\partial\theta}\ln\pi\right) + G_b S_b \frac{\partial}{\partial\theta}\ln\pi + G_a\left(S_a\frac{\partial}{\partial\theta}\ln\pi + v_{a0}\right). \tag{18}$$

The continuity equation (10) for steady symmetric flow is

$$\frac{\partial}{\partial\theta}\left(\pi\int_0^1 v_\theta ds\right) = 0 \tag{19}$$

and implies

$$\pi\int_0^1 v_\theta ds = \text{constant}, \tag{20}$$

but since the mass flux across a meridional circle must be zero and $\pi \neq 0$

$$\int_0^1 v_\theta ds = \text{Im}\int_0^1 v ds \equiv Av = 0 \tag{21}$$

where A represents taking the imaginary part of the integration over σ.

Now using (18) in (21) the solution for the gradient of the surface pressure is obtained;

$$\frac{\partial}{\partial\theta} \ln \pi = -\frac{AG\left(\frac{\partial\Phi}{\partial\theta}\right) + AG_a v_{a0}}{AG(T) + AG_b S_b + AG_a S_a}. \tag{22}$$

Then substituting (22) into (18) the velocity is solved for in terms of the applied temperature field. Thus, equations (18) and (22) represent the solution to the zero order dynamic problem once the polar symmetric temperature field and the boundary conditions have been defined.

4. Temperature field and Boundary Conditions

The dimensionless temperature field is assumed to be of the form

$$T_0 = T_s + (T_t + T_1 P_1(\theta) + T_2 P_2(\theta))\,\sigma^{\gamma} \tag{23}$$

where P_1 and P_2 are first and second degree Legendre polynominals of the first kind. T_s represents the stratospheric temperature, T_t is the globally averaged temperature at the surface and $T_1 P_1$ and $T_2 P_2$ are the equatorially symmetric and asymmetric parts respectively.

From equations (11) and (23) and with a prime on the Legendre function indicating differentiation with respect to θ the colatitudinal derivative of the geopotential function is

$$\frac{\partial\Phi}{\partial\theta} = (T_1 P_1' + T_2 P_2')\,\frac{1-\sigma^{\gamma}}{\gamma} + \frac{\partial\Phi_1}{\partial\theta}. \tag{24}$$

We shall assume that $\sigma = 1$ is a constant geopotential surface and define $\Phi_1 = 0$. Obviously, polar symmetric topology for which all the assumptions made are still valid can easily be treated, but topology will be considered in a subsequent paper.

Equation (24) gives the temperature and surface geopotential contributions to (18) and (22) and all that is required to complete the solution is the velocity boundary conditions.

At the surface the boundary condition will be imposed on the velocity alone by taking $\sin \alpha_b = 0$ and $v(1) = v_b$ in (16b). The surface velocity v_b is assumed to obey the equation

$$\xi \underline{k} \times \underline{v}_b + T_b \nabla \ln \pi + \delta \underline{v}_b = 0. \tag{25}$$

where T_b is obtained from (23) with $\sigma = 1$ and δ is a damping coefficient.[1] Defining the complex velocity $v_b = v_{b\phi} + i v_{b\theta}$ the solution to (25) is

$$v_b = T_b \frac{\xi - i\delta}{\xi^2 + \delta^2} \frac{\partial}{\partial \theta} \ln \pi \tag{26}$$

and from the relationship between v_b and S_b given preceeding (18)

$$S_b = T_b \frac{\xi - i\delta}{\xi^2 + \delta^2} . \tag{27}$$

[1] If we assume the eddy viscosity in a shallow boundry layer of depth z_b is equal to $k U_* Z$, where k is von Karman's constant, U_* the friction velocity and z the altitude (Monin and Yaglom, 1971), then by dimensional argument $\partial / \partial z \, (kU_* z \, \partial \underline{v}^* / \partial z) \sim k U_* / z_b \, \underline{v}_b U$ and $\delta = k U_* / 2 \Omega z_b$.

At the top of the atmosphere the two most reasonable choices of boundary conditions are to make the velocity geostrophic or impose a condition of zero shear. As $\sigma_0 \to 0$ the two are equivalent. Therefore (16a) with $v_a = 0$ and $\cos \alpha_a = 0$ will satisfy the shear condition exactly and the geostrophic condition very closely when σ_0 is very small. We can in fact take the top off the atmosphere and let $\sigma_0 = 0$ and both conditions will be satisfied. The geostrophic condition leads to the existance of a singularity in the velocity at $\sigma = 0$ in the equatorial plane, but the behavior in regions away from the singularity is not grossly affected and the pathological behavior at high altitudes in the equatorial plane will be tolerated. With v_a equal to zero, both v_{a0} and S_a appearing in (18) and (22) are identically zero.

Having defined the temperature field and the boundary conditions the surface pressure and wind fields can be calculated. Substituting (23) and (24) into (22) and (18) we get

$$\frac{\partial}{\partial\theta} \ln \pi = -\frac{1}{\gamma} \frac{(T_1 P_1' + T_2 P_2') \left[AG(1) - AG(\sigma^\gamma)\right]}{T_s AG(1) + (T_t + T_1 P_1 + T_2 P_2) AG(\sigma^\gamma) + AG_b S_b} \tag{28}$$

and

$$v = (T_1 P_1' + T_2 P_2') \frac{G(1) - G(\sigma^\gamma)}{\gamma} + \left[T_s G(1) + (T_t + T_1 P_1 + T_2 P_2) G(\sigma^\gamma) + G_b S_b\right] \frac{\partial}{\partial\theta} \ln \pi. \tag{29}$$

Using the definition of the operators G and A and the function G_b all the terms of (28) and (29) are easily calculated and the horizontal velocity and the surface pressure are expressed in terms of the Ekman number, the parameters of the

temperature field and the damping coefficient. The vertical velocity is calculated from (10) using the results obtained in (28) and (29).

The first order temperature field can be calculated from equation (13) after the zero order velocities have been determined. Designating the terms in the brackets on the right hand side of the equation by Q_D and neglecting the horizontal diffusion term, the first order equation is

$$\sigma^2 \frac{\partial^2 T_\beta}{\partial \sigma^2} + (2 - \kappa)\,\sigma \frac{\partial T_\beta}{\partial \sigma} - (\kappa + \delta_T)\, T_\beta = -\frac{P}{\epsilon} Q_D \qquad (30)$$

where

$$\delta_T = \frac{P}{(\tau \epsilon)} .$$

Assuming T_β is zero at $\sigma = \sigma_0$ and $\sigma = 1$, (30) is solved in a manner similar to (15). The details are given in Appendix II.

5. Numerical Results

In applying the analysis of the preceeding sections three values of eddy viscosity $K_M = 10^6$, 10^7 and 10^8 cm^2/sec ($\epsilon = .006$, .06 and .6) are used to represent what might be from slightly to extremely unstable conditions in the atmosphere. With each value of eddy viscosity two surface boundary conditions are considered, the conditions being no-slip ($v_b = 0$) or the surface velocity controlled by a linear damping term as indicated in (29). The latitudinal behavior of the surface pressure is calculated under the six combinations of viscosity and boundary conditions for a model of a temperature field based on the Mariner 9 infrared spectrometer data (Hanel, et al, 1972).

The vertically averaged temperature is shown in the top part of Figure 1. In accordance with (23) the temperature field is $T = 150 + (395/6 - 45/2 P_1 - 85/3 P_2)\sigma^{.45}$. The parameters chosen give temperatures of 150°, 165°, 230° and 210° Kelvin in the stratosphere and at the base of the atmosphere at the north pole, equator and south pole respectively. This roughly approximates the diurnally averaged Martian atmospheric temperatures during the dissipation of the dust storm (Hanel, et al, 1972). The two lower parts of Figure 1 show the ratios of surface pressure to globally averaged surface pressure associated with the three values of eddy viscosity for both boundary conditions. From each section of the figure the dependence of the pressure on viscosity is apparent while in all cases its latitudinal behavior is opposite that of the vertically averaged temperature.

The reason for the increase in the pressure gradient resulting from an increase in eddy viscosity can be seen from a simplification of (28). Assuming that the vertical and horizontal temperature variations are small compared to T_s and neglecting the boundary term since it is not essential to the argument, (28) can be expressed as

$$\frac{\partial}{\partial\theta} \ln \pi = - \frac{T_1 P_1' + T_2 P_2'}{T_s} \frac{\mathrm{Im} \int_0^1 S^{-1/2\,(1-x)}\, \frac{1 - S^\gamma}{\gamma}\, ds}{\mathrm{Im} \int_0^1 S^{-1/2\,(1-x)}\, ds}, \qquad (31)$$

where $\mathrm{Im}\, S^{-1/2\,(1-x)}$ can be viewed as weighting function. The vertical behavior of the geopotential function $(1 - S^\gamma)/\gamma$ and the weighting function at 45° latitude for $K_M = 10^6$, 10^7 and 10^8 cm^2/sec are shown in Figure 2. With the integral in the denominator acting as a normalizing factor and the numerator being the integrated product of the weighting and geopotential functions, the more overlap

between the two functions the larger the quotient of the two integrals will be. Thus it is apparent from Figure 2 that larger pressure gradients are associated with larger viscosities. The weighting function is a measure of the thickness of the viscous dominated boundary layer. If $\epsilon << 4\xi$ the weighting function is of the form $\sigma^{\sqrt{\xi/(2\epsilon)}} \sin(\sqrt{\xi/(2\epsilon)} \ln\sigma)$ and has a negative one-half power Ekman number behavior. Larger eddy viscosities cause thicker boundary layers in which an increase mass of the atmosphere is freed from geostrophic flow and has a meridional component. The increased shear resistance due to the larger viscosity coupled with the greater mass in nongeostrophic flow results in an increased pressure gradient.

Note also that the parameter γ in the geopotential function has an effect on the pressure gradient. Large values of γ yield small pressure gradients through the decrease of the effective depth of the atmosphere in which a horizontal temperature gradient drives the circulation. To the zero order the effect on surface pressure is not due to a change in the stratification and it is a different effect than that discussed in Barcilon and Pedlosky (1967a, b). We have implicitly assumed that eddy diffusion overwhelms convection and the flow is essentially that of a homogeneous fluid as opposed to stratified flow (Greenspan, 1968, 124-132) as pointed out above. However, if the vertical temperature gradient is sufficiently large, the higher order terms must be considered as was also pointed out above.

Comparing the no-slip cases to the cases in which a surface velocity is permitted indicates that the type of boundary condition also has an appreciable effect on the surface pressure. The essentially smaller flow resistance in the

cases with non-zero surface velocity allows more mass flow near the surface resulting in less piling up of the atmosphere at the poles and, consequently, a smaller surface pressure gradient. The upper atmosphere tends to flow towards the poles due to the downward slope of the constant pressure surfaces towards the colder parts of the atmosphere while the surface pressure gradient causes a return flow from the poles to the subsolar region.

Figure 3 indicates the rate at which the cellular flow turns over the atmosphere in the no-slip and finite surface velocity cases. Plotted for three values of eddy viscosity is the percentage of the atmosphere that is exchanged across a latitudinal circle normalized to the circumference of the latitudinal circle. The large flow rates in the equatorial region for K_M equal to 10^6 and 10^7 are not correct since for these cases both ϵ and ξ are small and the non-linear β order terms should be included since all the velocity terms of (9) may be of the same magnitude. Outside of the equatorial region where the coriolis term is of appreciable magnitude, the results are a good approximation for all the values of eddy viscosity.

In regions away from the equator there is approximately a tenfold increase in the flow in going from $K_M = 10^6$ to $K_M = 10^8$ cm^2/sec. The implications of this increase and the flow rates will be addressed later.

The cellular flows associated with the different values of eddy viscosity are shown in Figures 4, 5, and 6. The atmosphere rises in the latitudinal band of maximum temperature and descends at the poles, while associated with this motion is a zonal flow generally geostrophic at high altitudes and oppositly directed in the boundary layer which causes an atmospheric parcel to spiral towards and away from the poles, the exact nature depending upon the viscosity

and the boundary conditions. As stated previously, the results in the equatorial region are a poor approximation for $K_M = 10^6$ and 10^7 cm^2/sec. The increased meridional flow associated with a finite surface velocity is apparent when comparison is made between the no-slip and finite surface velocity conditions indicated in Figure 3.

A comparison between Figures 4, 5 and 6 indicates the effect of the viscosity and consequently the boundary layer thickness upon the cellular flow. The pole to subsolar latitude flow takes place in the boundary layer while the subsolar latitude to pole flow is in a region of approximate geostrophic flow as seen from Figure 7. A change in viscosity changes both the altitude at which the north-south flow changes direction and the latitude at which the ascending-descending flow changes direction.

Figures 7 and 8 show some representative wind profiles. Figure 7 illustrates the magnitude and direction of the horizontal flow at 40° north and south for three values of eddy viscosity and zero-slip boundary conditions. Figure 8 illustrates the analogous information for the boundary condition which allows a finite surface velocity based on one day damping, $\delta = .5/\Omega$. Figures 4 through 6 indicate that there is always a small meridional flow except at $\sigma = 0$ where the flow is geostrophic, while from Figures 7 and 8 the layers through which geostrophic flow is dominant are clearly shown from the plots of the directions. Geostrophic flow is indicated by the east direction and in Figures 7 and 8 it is seen to dominate the upper 4/5 of the atmosphere when $K_M = 10^6 cm^2/sec$ and the upper 1/2 and 1/10 when $K_M = 10^7$ and 10^8 cm^2/sec respectively. The thickness of the outer boundary layer depends upon the Ekman number and is independent of the inner boundary condition as is evident from the comparison of Figures 7 and 8. It

should be pointed out that the thickness also depends upon the latitude because in the Green's function, which determines the influence of adjacent layers upon one another, there appears exponents of σ containing the term ξ/ϵ. Decreasing the distance from the equator (decreasing ξ) is equivalent to increasing the eddy viscosity (increasing ϵ) and subsequently increasing the boundary layer thickness.

While the thickness of the boundary layer is unaffected by the boundary condition, the behavior within the layer is changed markedly with a change in boundary conditions. For example, when $K_M = 10^7 cm^2/sec$ and a zero-slip boundary condition is imposed, the wind vector rotates counter-clockwise through approximately 90° with increasing altitude, as seen in Figure 7. When a surface velocity is permitted, as in Figure 8, the wind vector rotates clockwise through approximately 120°. In addition, when a surface velocity is permitted, in going from $K_M = 10^6$ to $K_M = 10^7$ cm^2/sec the wind vector rotates in opposite directions.

Outside the boundary layer the wind profiles for each value of eddy viscosity are all similar and are dependent upon the temperature field and only weakly dependent on the boundary conditions through the differences in surface pressures.

Assuming a Prandtl number equal to unity the first order temperature field was calculated for a variety of conditions. A sketch of the general form of the isotherms representative of all the cases is shown in Figure 9. Figures 10 and 11 show temperature profiles at ±40° latitude for the three values of eddy viscosity used previously and with radiative damping times of one and ten days. The results shown are for a no-slip surface boundary condition. Having chosen a Prandtl number equal to unity, $K_H = K_M$ and $\epsilon = K_M/(2\,\Omega\,H^2) = K_H/(2\,\Omega\,H^2)$.

The parameter ϵ appears explicitly as a coefficient in the equation for the first order temperature in Appendix II and implicitly through h_1, h_2, J_h and the heating term Q_D. Thus, as is apparent from Figures 10 and 11, the dependency of the temperature on the eddy viscosities is not simple. In the regions poleward of 30° the effect of the smaller vertical velocity in decreasing the temperature is partially offset by a decrease in heat diffusion, both being the result of smaller eddy diffusion terms.

Comparison of Figures 10 and 11 indicate the larger first order temperature associated with a decrease in the radiative damping.

When the eddy viscosity is 10^6 or 10^7 cm^2/sec the maximum and minimum temperatures are of the order of tens of degrees and occur at high altitudes in regions of large vertical velocities seen in Figures 5 and 6. For reasons stated earlier these results are unrealistic since the nonlinear terms should be considered and the large gradients would have a significant effect on the dynamics, but only within a limited region. With an eddy viscosity of 10^8 cm^2/sec, the minimum and maximum temperatures are -8 to +4 K for $\tau^* = 1$ and -10 to +5 K for $\tau^* = 10$ and the gradients associated with these temperatures would not have a significant effect on the dynamics. The main aspects of the flow would remain unchanged.

6. Discussion of Results

Evidently a better description of the behavior of eddy viscosity with altitude and an improved simulation of boundary conditions are needed in order to give a better description of the wind profile, especially in the boundary layer, and without a more definitive description of the radiative effects, it is difficult to

predict the temperature field in anything more than a qualitative manner. More sophisticated models could have been used in the analysis but would have unduly complicated the calculations at this stage of its development. In spite of the simple treatment of the eddy viscosity and the boundary conditions, the latitudinal pressure gradient and meridional flow rate are obviously correlated with the boundary condition imposed at the surface and the vertical stability of the atmosphere as manifested in the eddy viscosity. In addition, the mechanism for a polar temperature inversion is present.

For large values of eddy viscosity, the geostrophic approximation is a poor one for the bulk of the atmosphere, but when the eddy viscosity is of the order of 10^6 cm^2/sec or less the geostrophic approximation should be adequate if one is concerned with the bulk of the atmosphere and not with the boundary layer. As the equator is approached the approximation becomes poorer because the boundary layer increases in thickness as pointed out above.

The dependence of the rate of overturning of the atmosphere on the eddy viscosity has implications in the evolution of the great dust storm observed by the Mariner 9 experiments at the time of the spacecraft's arrival at Mars in November of 1971. (See the October 1972 issue of Icarus which is devoted primarily to results obtained from Mariner 9 and Mars 2 and 3.) The dust storm appears to have started about the time of maximum solar insolation which, assuming that at that time the atmosphere was relative clear of dust, was on the average a time of strong convective instability. Although the temperature model used is supposedly representative of conditions during the dissipation of the dust storm it may well represent the temperature structure during the growth of the storm. In any event it will suffice for our argument since the

flow rates would not suffer an order of magnitude change with any reasonable alteration of the temperature field. If the average eddy viscosity were as large as 10^8 cm^2/sec our model predicts a complete overturning of the atmosphere on the order of tens of days. This is consistent with the ground based observations indicating a global spreading of the storm in approximately 15 days. When dust becomes entrained in the atmosphere, the direct solar heating increases (Gierasch and Goody, 1972) and the convective instability decreases. There is evidence of this behavior indicated by the increasing lapse rate as the atmosphere was clearing as observed by the infrared interferometer on Mariner 9 (Hanel, et al, 1972). Conrath (1974) shows that an eddy viscosity of 10^7 cm^2/sec is consistent with the settling rate of the dust inferred by the secular variation of the temperature. If the eddy viscosity decreases to 10^6 cm^2/sec or less, the time of overturning increases to hundreds of days. Thus, the most elementary mode of the global dynamics appears to augment the processes that cause the sudden growth and slow decay of the dust storm.

If the boundary conditions allow a velocity, as indicated in (32), the surface winds directions are similar to the diurnal average of the near surface winds shown in Pirraglia and Conrath (1974), which isn't surprising since both are calculated in the same way. When the boundary layer is simulated by a thin layer in which the viscosity is less than the viscosity of the upper layer, the same type of wind pattern as mentioned above is obtained at the interface. In the equatorial region this agrees rather well with the wind blown streaks seen in the Mariner 9 television pictures (Sagan, et al, 1973). When a zero shear boundary condition is used at the surface of the planet the surface pressure, while still having the same qualitative behavior as before, then has a magnitude

independent of the eddy viscosity. The pressure is in fact identical to that found using linear damping. The surface wind magnitude and direction are viscosity dependent but nevertheless always lie in the quadrant giving general agreement with the Mariner 9 television pictures.

We have compared our results with the numerical study of Leovy and Mintz (1969) and there is a qualitative agreement of surface pressures in the $\pm 35^\circ$ latitude zone. The disagreement is at the poles, due to their including condensation and sublimitation of the atmosphere, which could be incorporated into our model, and in the regions of baroclinic instability, which requires an extension of our analysis to somehow parameterize the effect.

The approach presented did not consider the nonlinear terms or the possibility of instabilities. In the limit of a very small Rossby number the results should be a good approximation to the symmetric flow. Nevertheless, at this time we do not know whether or not our model falls in the region of Rossby-Ekman number parameter space where instabilities occur, assuming similarities between a rotating sphere and the "qualitatively inferred" experimental results shown in Robinson (1959) which indicate symmetrical stable, wave and eddy regimes.

ACKNOWLEDGEMENTS

The author is grateful to Dr. B. J. Conrath for the many helpful discussions, to Dr. R. A. Hanel for the suggestions concerning both the subject of this paper and related areas, and to Prof. P. J. Gierasch for his comments. Part of the work presented was performed during the author's tenure as a National Academy of Sciences Resident Research Associate at NASA's Goddard Space Flight Center.

APPENDIX I

The solutions to the homogeneous form of (15) designated by w_1 and w_2, w_1 satisfying the homogeneous boundary condition at $\sigma = \sigma_0$ and w_2 satisfying the condition at $\sigma = 1$, are

$$w_1 = \sigma^{-1/2\,(1-\chi)} + c_a \sigma^{-1/2\,(1+\chi)}$$

$$w_2 = \sigma^{-1/2\,(1-\chi)} + c_b \sigma^{-1/2\,(1+\chi)}$$

where

$$c_a = \frac{(1-\chi)\,\sigma_0^{-1} \sin \alpha_a - 2 \cos \alpha_a}{2 \cos \alpha_a - (1+\chi)\,\sigma_0^{-1} \sin \alpha_a}\,\sigma_0^{\chi}$$

$$c_b = \frac{(1-\chi) \sin \alpha_b - 2 \cos \alpha_b}{2 \cos \alpha_b - (1+\chi) \sin \alpha_b}$$

and $\chi = \sqrt{1 - 4i\xi/\epsilon}$. The conjunct of w_1 and w_2 is defined by

$$J = -i\epsilon\sigma^2 (w_2' w_1 - w_1' w_2) = i\epsilon (c_b - c_a)\,\chi$$

where the prime indicates differentiation with respect to σ. If the solutions w_1 and w_2 are linearly independent then the conjunct J is independent of σ. In terms of the homogeneous solutions the solution to the inhomogeneous equation (15) is

$$v(\sigma, \theta) = \frac{w_2(\sigma, \theta)}{J(\theta)} \int_{\sigma_0}^{\sigma} w_1(s, \theta) F(s, \theta) ds + \frac{w_1(\sigma, \theta)}{J(\theta)} \int_{\sigma}^{1} w_2(s, \theta) F(s, \theta) ds$$

$$+ i\epsilon v_b w_1(\sigma, \theta) \frac{w_2(1) \sin \alpha_b - w_2'(1) \cos \alpha_b}{J(\theta)}$$

$$- i\epsilon \sigma_0^2 v_a w_2(\sigma, \theta) \frac{w_2(J_0) \sin \alpha_a - w_1'(\sigma_0) \cos \alpha_a}{J(\theta)}$$

where the integrals represent the Green's function solution for homogeneous boundary conditions and the third and fourth terms are the contributions of the inhomogeneous boundary condition (see Friedman, 1965).

The solution is dependent upon the choice of the eddy viscosity term (1) and the particular choice leads to a relatively simple solution but, in fact, the eddy viscosity terms can be more general and lead to more complicated solutions than used here.

APPENDIX II

The homogeneous solutions to (30) are

$$h_1 = \sigma^{-D-} - \sigma_s^{\sqrt{(1+\kappa)^2+4\delta_T}}\,\sigma^{-D+}$$

$$h_2 = \sigma^{-D-} - \sigma^{-D+}$$

where

$$D_+ = \frac{1}{2}\left[1 - \kappa + \sqrt{(1+\kappa)^2 + 4\delta_\gamma}\right]$$

$$D_- = \frac{1}{2}\left[1 - \kappa - \sqrt{(1+\kappa)^2 + 4\delta_T}\right].$$

At both $\sigma = 1$ and $\sigma = \sigma_0$ h_1 and h_2 are equal to zero. The conjunct of h_1 and h_2 is

$$J_T = -\sqrt{(1+\kappa)^2 + 4\delta_T}\;\left(1 - \sigma_0\sqrt{(1+\kappa)^2 + 4\delta_T}\right).$$

Using the homogeneous solutions to construct a Green's function, the solution to (30) is

$$T_\beta(\sigma, \theta) = \frac{P}{\epsilon J_T}\left[h_2(\sigma)\int_{\sigma_0}^{\sigma} h_1(s)\, s^{-\kappa} Q_D(s, \theta)\, ds + h_1(\sigma)\int_{\sigma}^{1} h_2(s)\, s^{-\kappa} Q_D(s, \theta)\, ds\right].$$

REFERENCES

Barcilon, V., and J. Pedlosky, 1967a; Linear theory of rotating stratified fluid motions. J. Fluid Mech., 29, 1-16.

Barcilon, V., and J. Pedlosky, 1967b; A unified linear theory of homogeneous and stratified rotating fluids. J. Fluid Mech., 29, 609-621.

Conrath, B. J., 1974; to be published.

Friedman, B., 1965; Principles and Techniques of Applied Mathematics, John Wiley & Sons, Inc., New York, 315 pp.

Gierasch, P. J. and R. M. Goody, 1972; The effect of dust on the temperature of the Martian atmosphere. J. Atmos. Sci., 29, 400-402.

Greenspan, H. P., 1968; The Theory of Rotating Fluids, Cambridge Univ. Press, London, 325 pp.

Hanel, R., et al., 1972; Investigation of the Martian environment by infrared spectroscopy on Mariner 9. Icarus, 17, 423-442.

Leovy, C. and Mintz, Y., 1969; Numerical simulation of the atmospheric circulation and climate of Mars. J. Atmos. Sci., 26, 1167-1190.

Monin, A. S. and A. M. Yaglom, 1971; Statistical Fluid Mechanics, MIT Press, Cambridge, 769 pp.

Phillips, N. A., 1957; A coordinate system having some special advantages for numerical forecasting. J. Meteor., 14, 184-185.

Pirraglia, J. A. and B. J. Conrath, 1973; Martian tidal pressure and wind fields obtained from the Mariner 9 infrared spectroscopy experiment. J. Atmos. Sci., 31, 318-329.

Robinson, A. R., 1959; The symmetric state of a rotating fluid differentially heated in the horizontal. J. Fluid Mech., 6, 599-620.

Sagan, C., et al., 1973; Variable features on Mars 2, global results. J. Geophys. Res., 78, 4163-4196.

Spiegel, E. A. and G. Veronis, 1960; On the Boussinesq approximation for a compressible fluid. Astrophys. J., 131, 442-447.

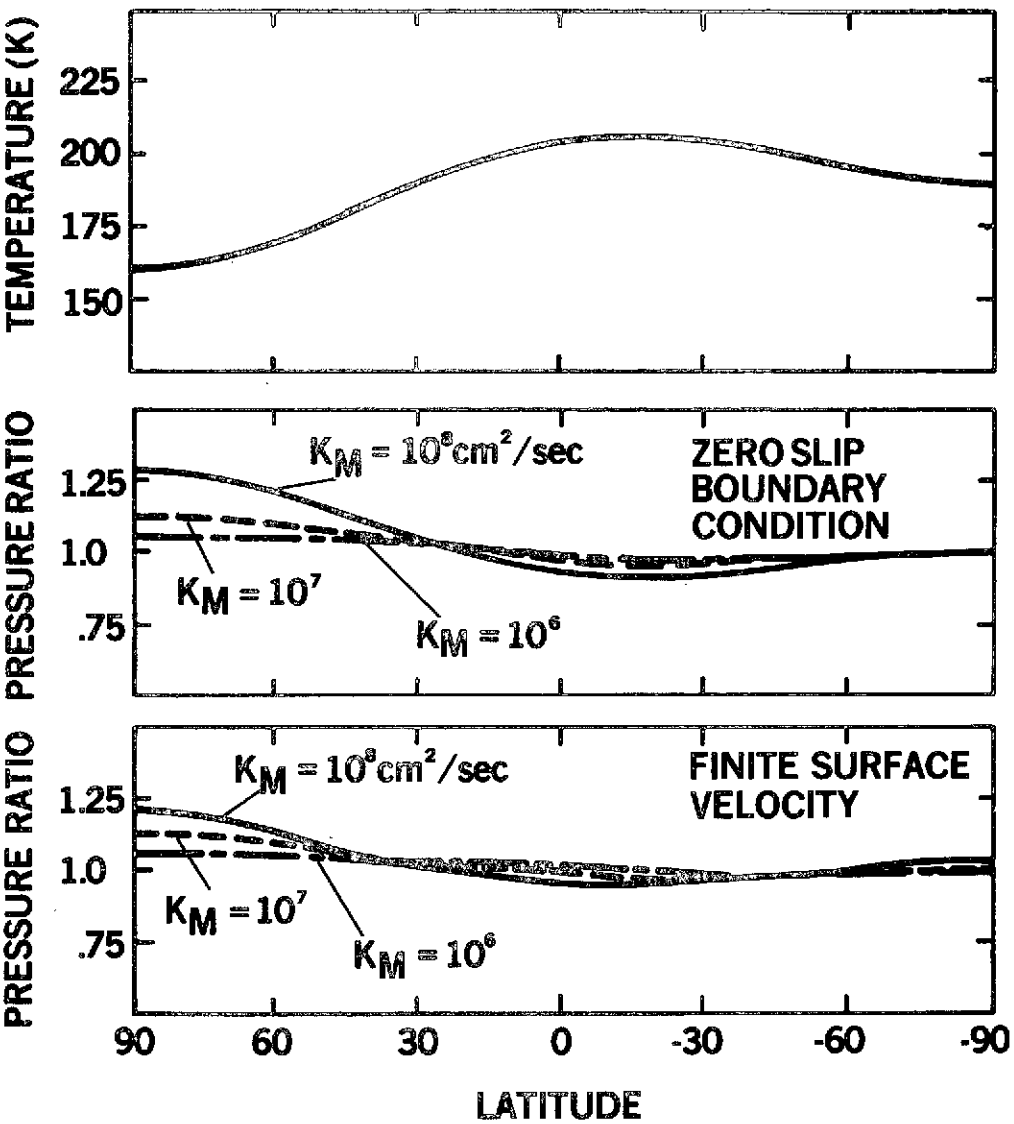

Figure 1. Depth averaged temperature and surface pressures vs latitude. Six conditions of eddy viscosity and surface boundary conditions are represented in the two lower sections of the figure.

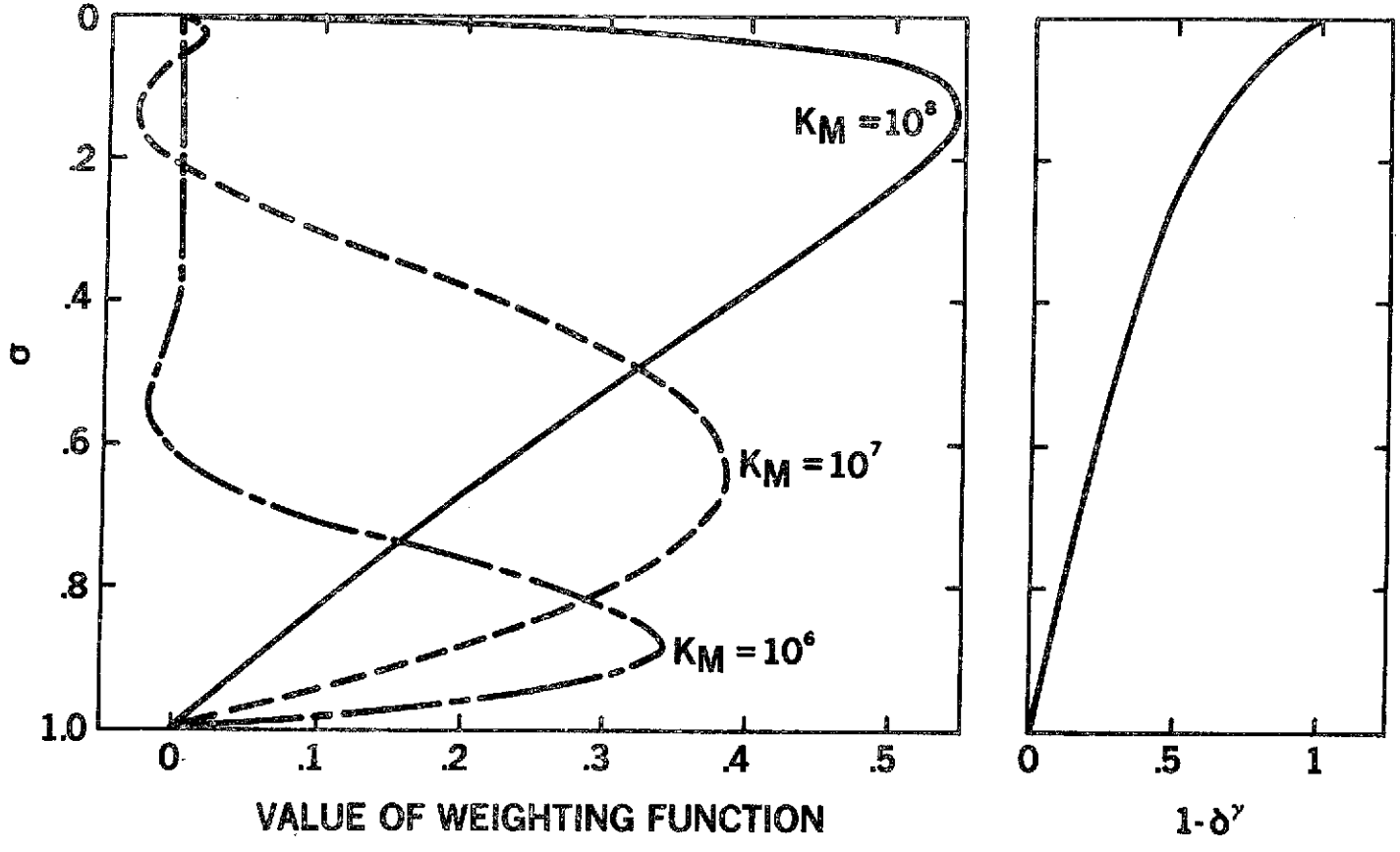

Figure 2. The influence of the boundary layer and the geopotential function vs altitude at 45° latitude. The surface pressure gradient is proportional to the quotient of the σ-integrated product of the geopotential and weighting functions, and the σ-integrated weighting function.

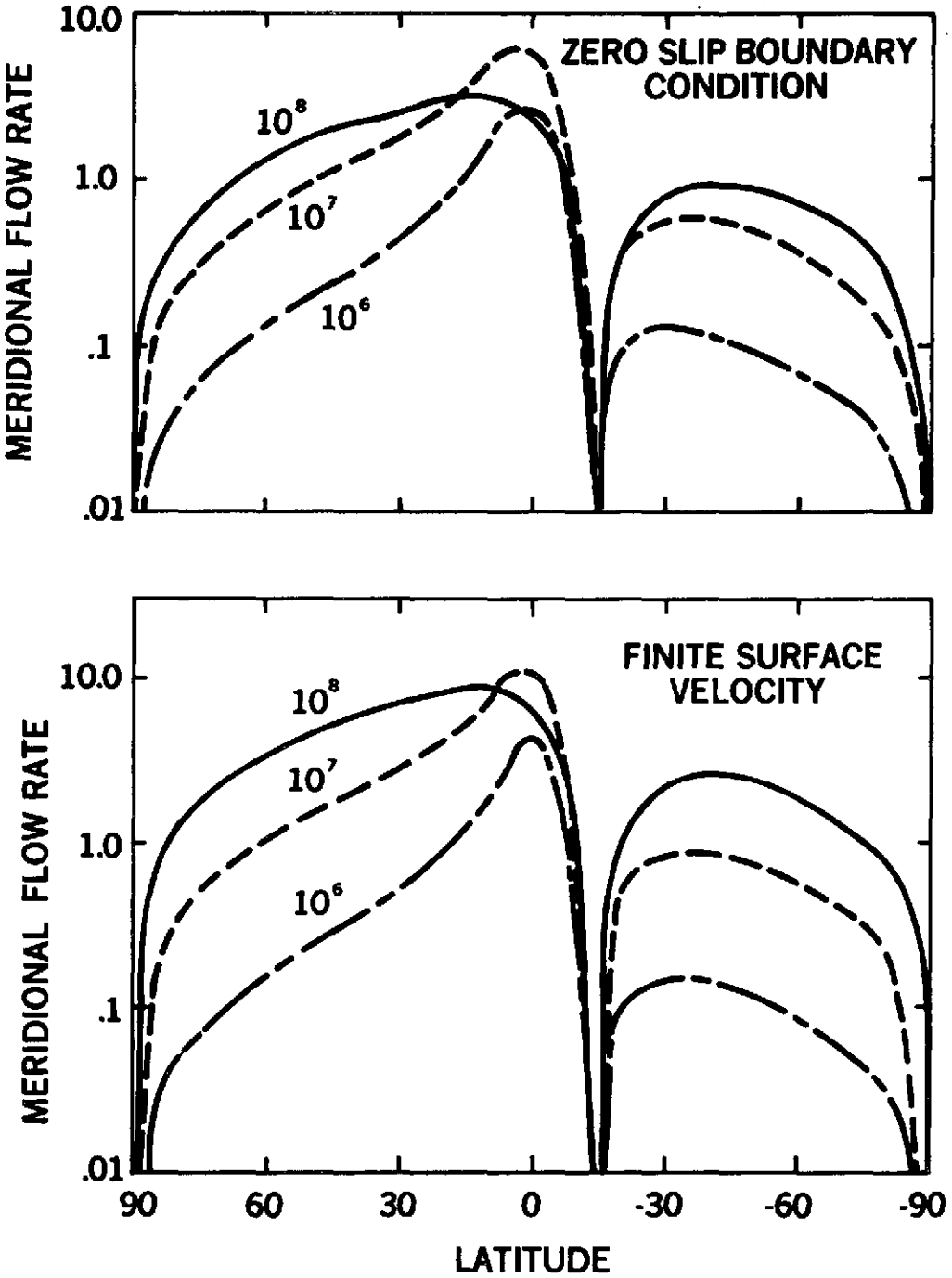

Figure 3. Meridional cell flow rates as a function of latitude for three values of eddy viscosity and two different boundary conditions. The flow rates represent the percentage of the total mass of the atmosphere that is exchanged across a latitudinal circle in one day normalized to the cosine of the latitude. In all cases, to the North of -20° the flow at the surface is to the South and South of -20° the flow is to the North.

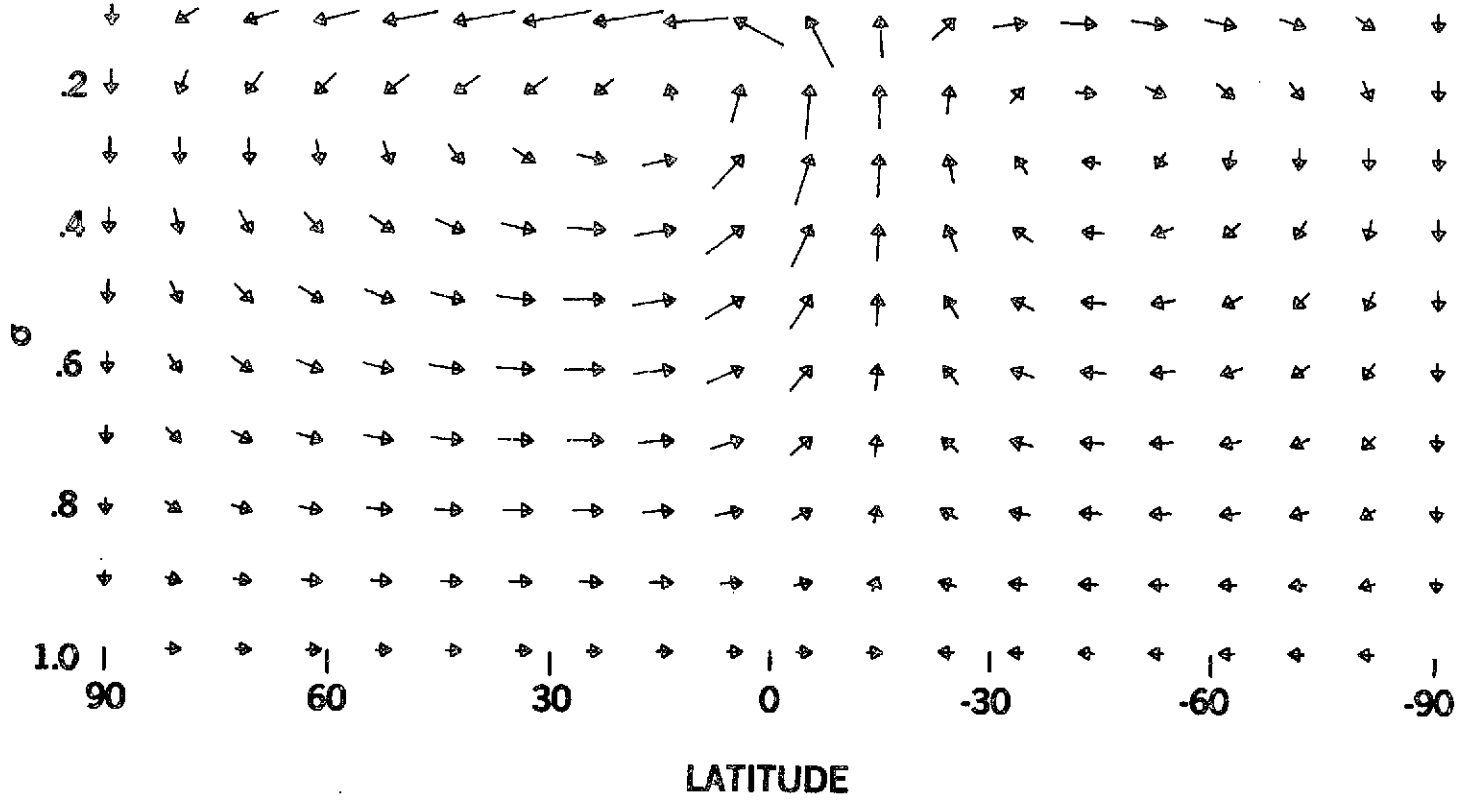

Figure 4. Cellular flow pattern with no-slip boundary conditions and $10^8 cm^2/sec$ eddy viscosity. An arrow length equal to the distance between arrow heads represents a velocity of 6.25m/sec in the horizontal direction and a velocity of $.2/\sigma$ cm/sec in the vertical direction.

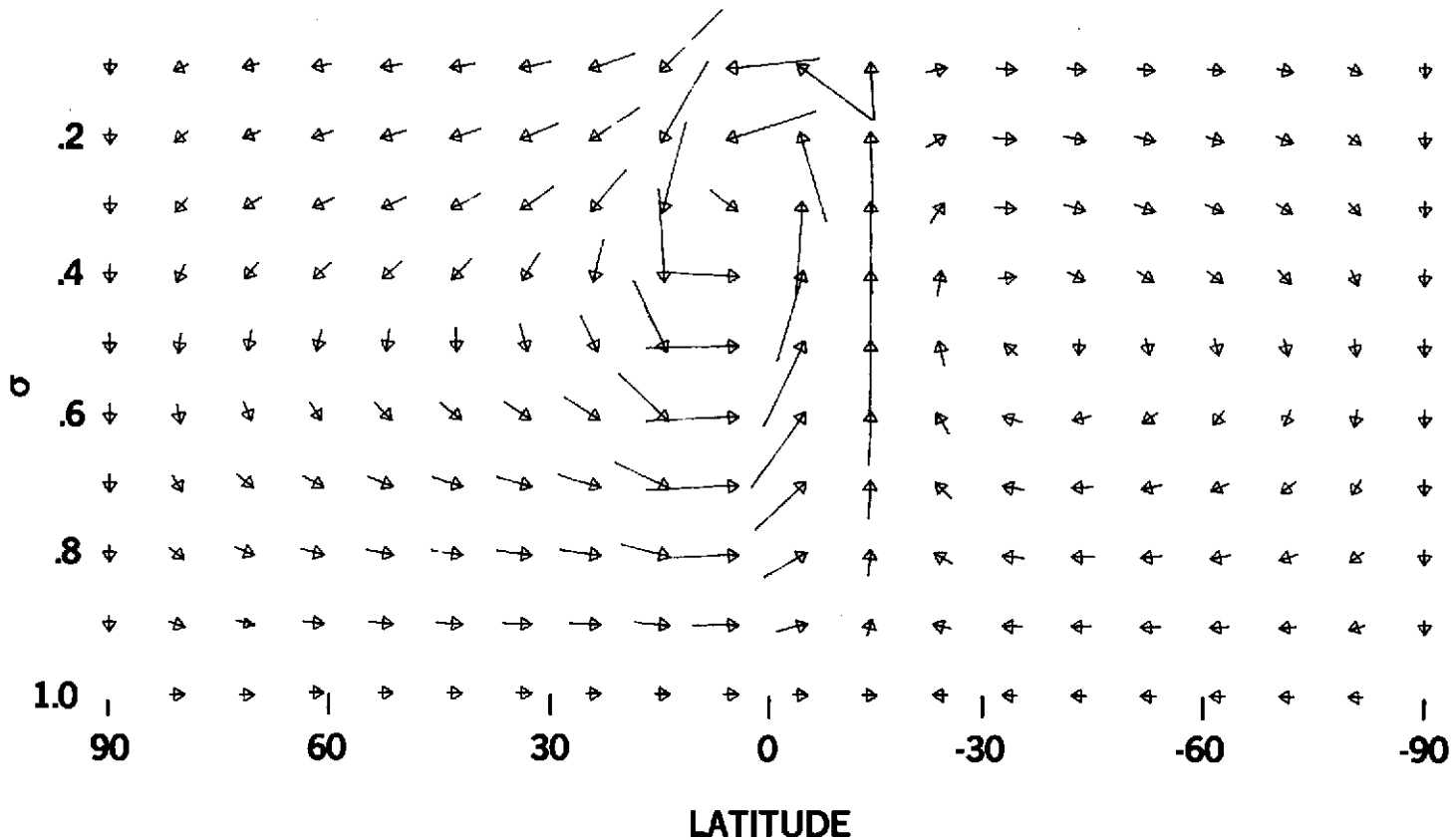

Figure 5. Cellular flow pattern with no-slip boundary conditions and 10^{7}cm^{2}/sec eddy viscosity. An arrow length equal to the distance between arrow heads represents a velocity of 6.25m/sec in the horizontal direction and a velocity of $.2/\sigma$ cm/sec in the vertical direction.

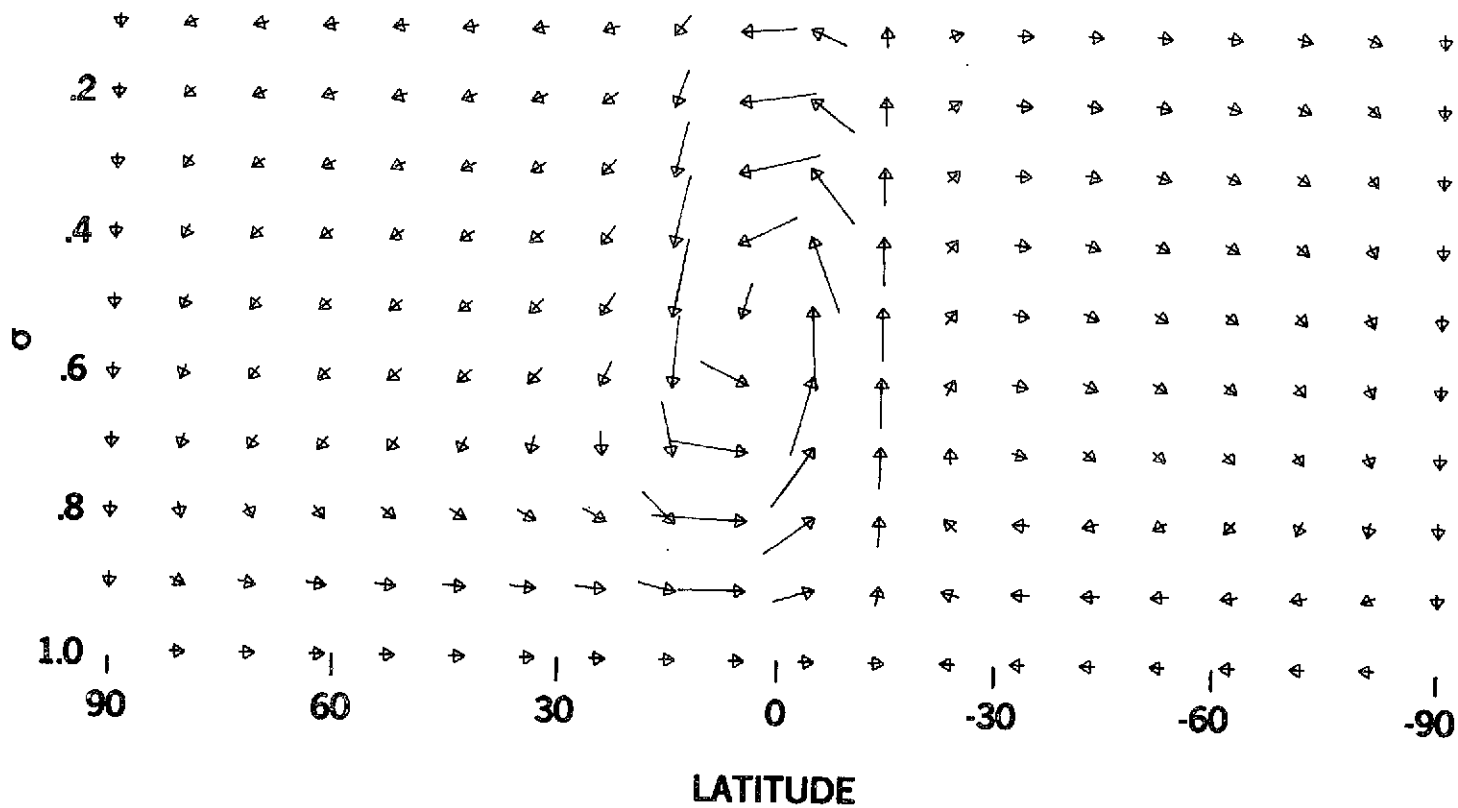

Figure 6. Cellular flow pattern with no-slip boundary conditions and $10^6 cm^2/sec$ eddy viscosity. An arrow length equal to the distance between arrow heads represents a velocity of 6.25m/sec in the horizontal direction and a velocity of $.2/\sigma$ cm/sec in the vertical direction.

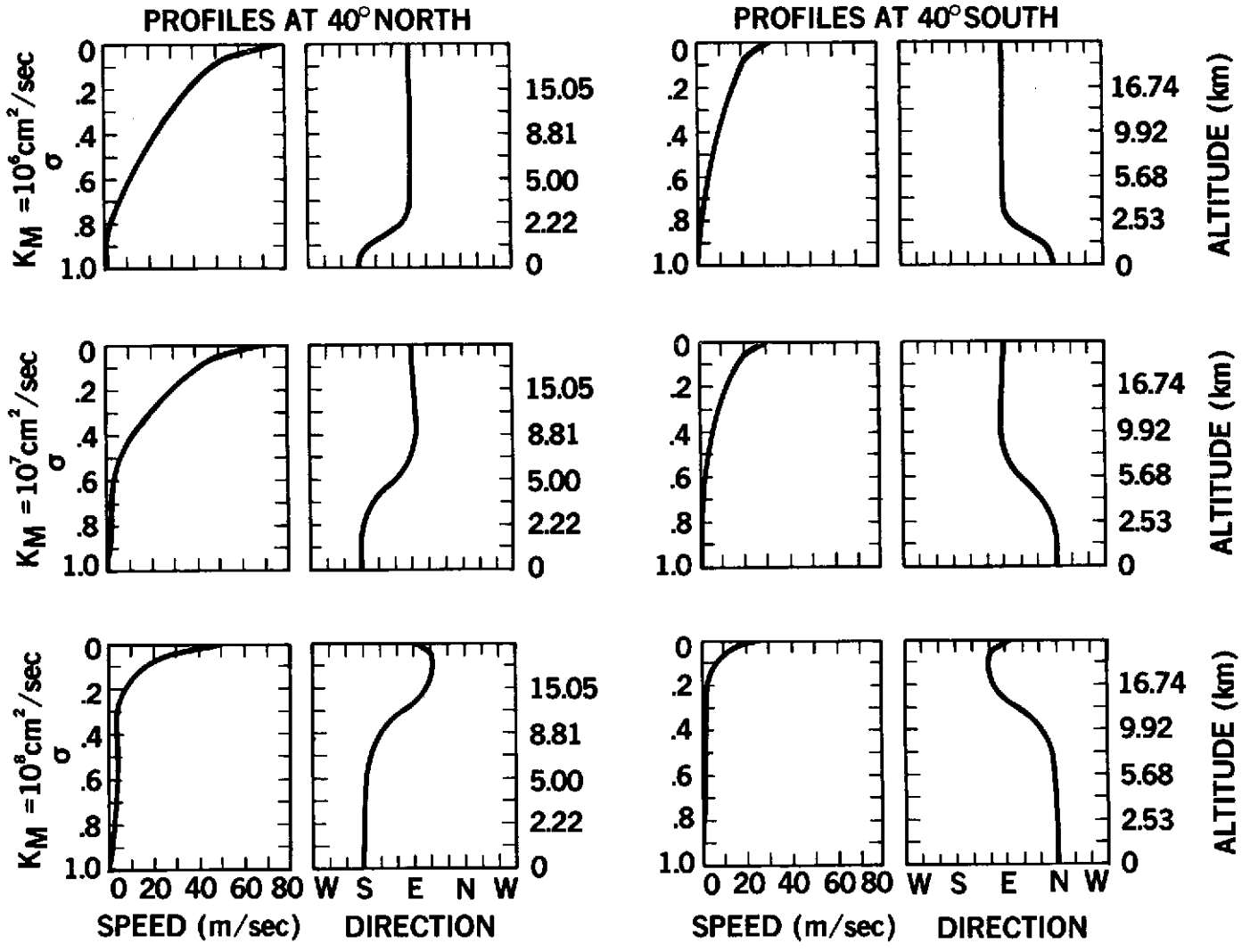

Figure 7. Wind profiles vs altitude at 40° North and South latitudes with eddy viscosities of 10^6, 10^7, and $10^8 cm^2/sec$ and no-slip boundary conditions imposed at the surface.

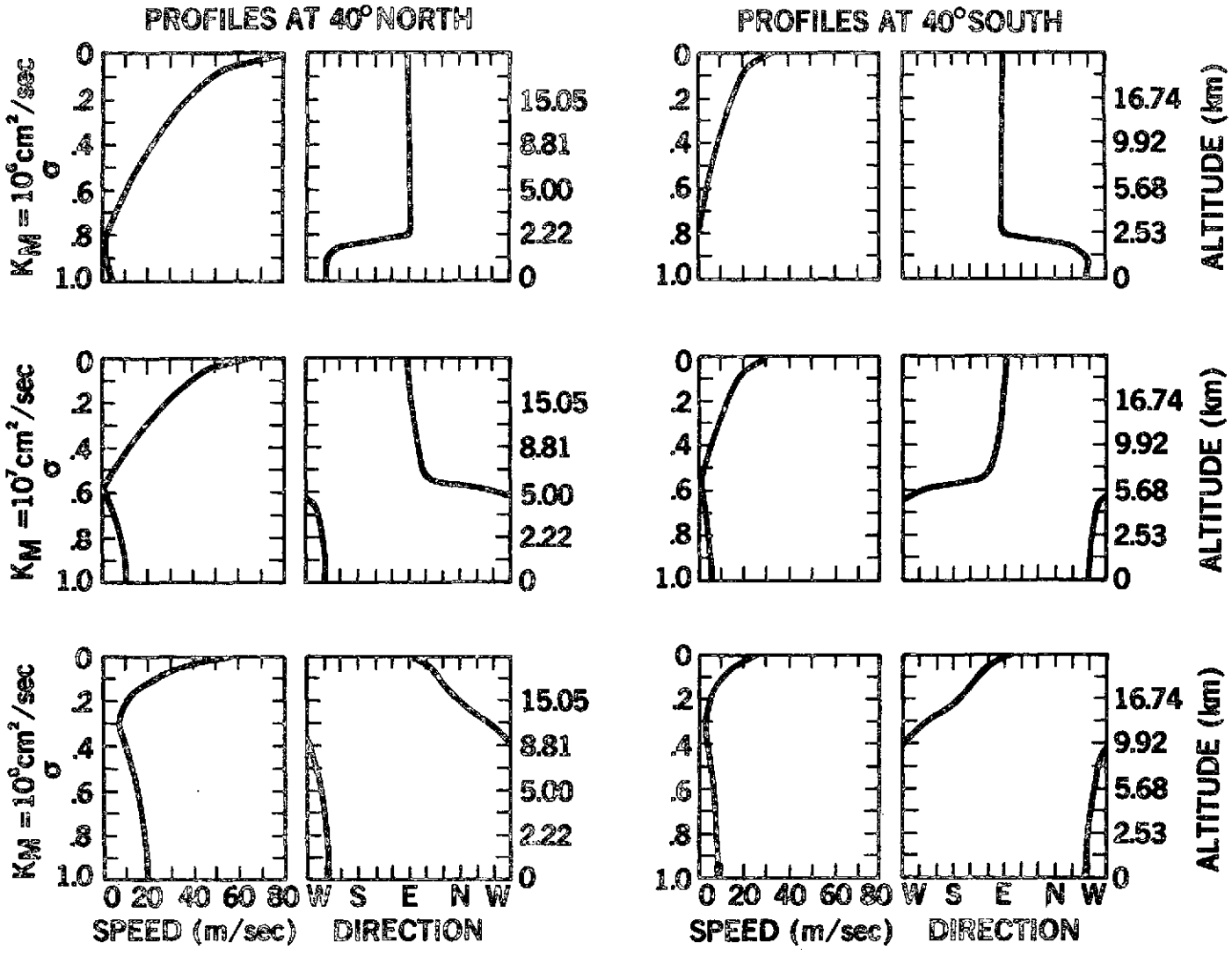

Figure 8. Same as Figure 7 but with a finite surface velocity as described in the text.

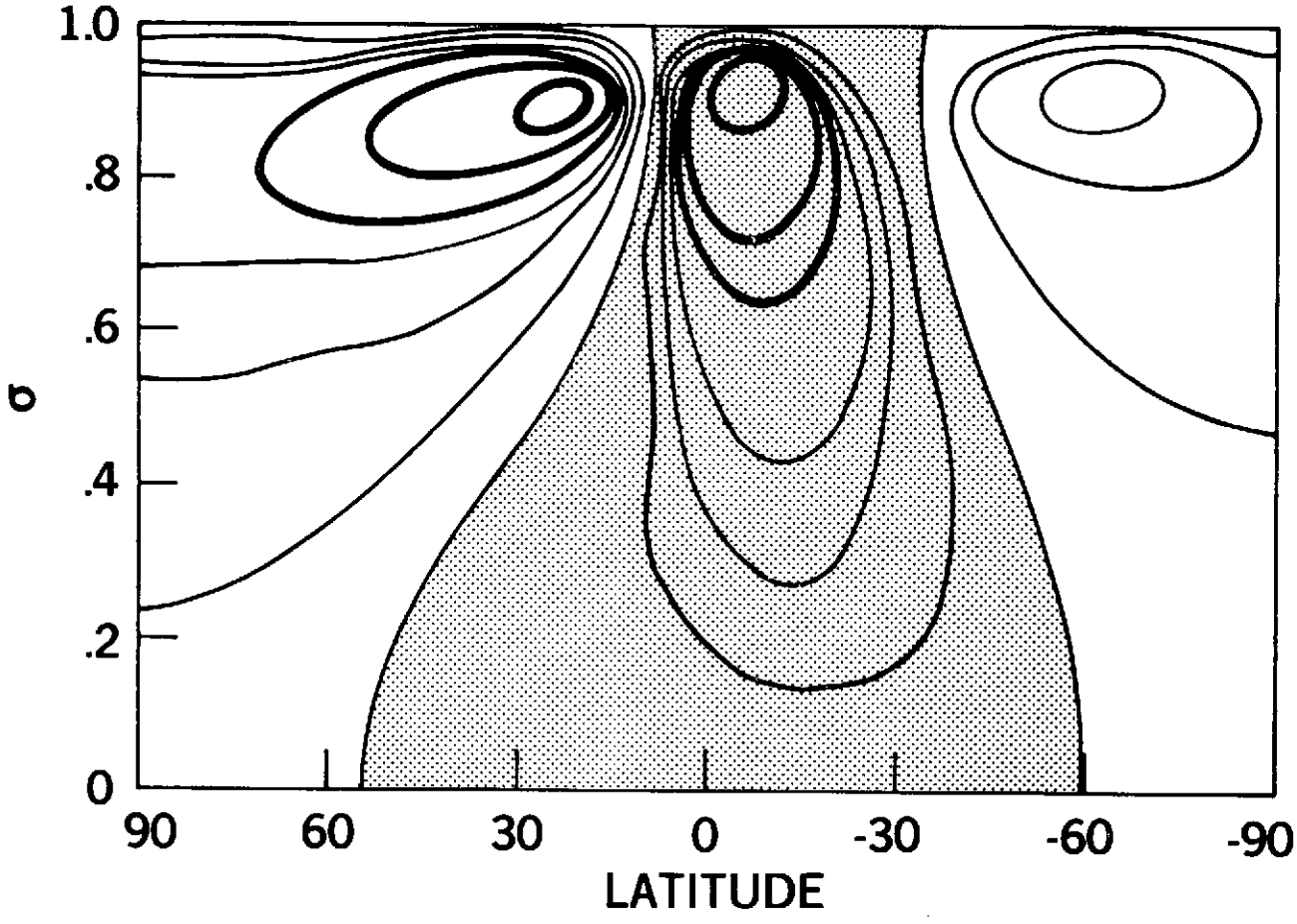

Figure 9. Isotherms of the first order temperature field. The shaded area is cooled, the rest is heated. The light lines represent .25K intervals the heavy lines 1.0K intervals. The figure is a sketch of the case with $K_M = K_H = 10^8 cm^2/sec$. For smaller values of eddy viscosities the form remains essentially the same while the magnitudes change.

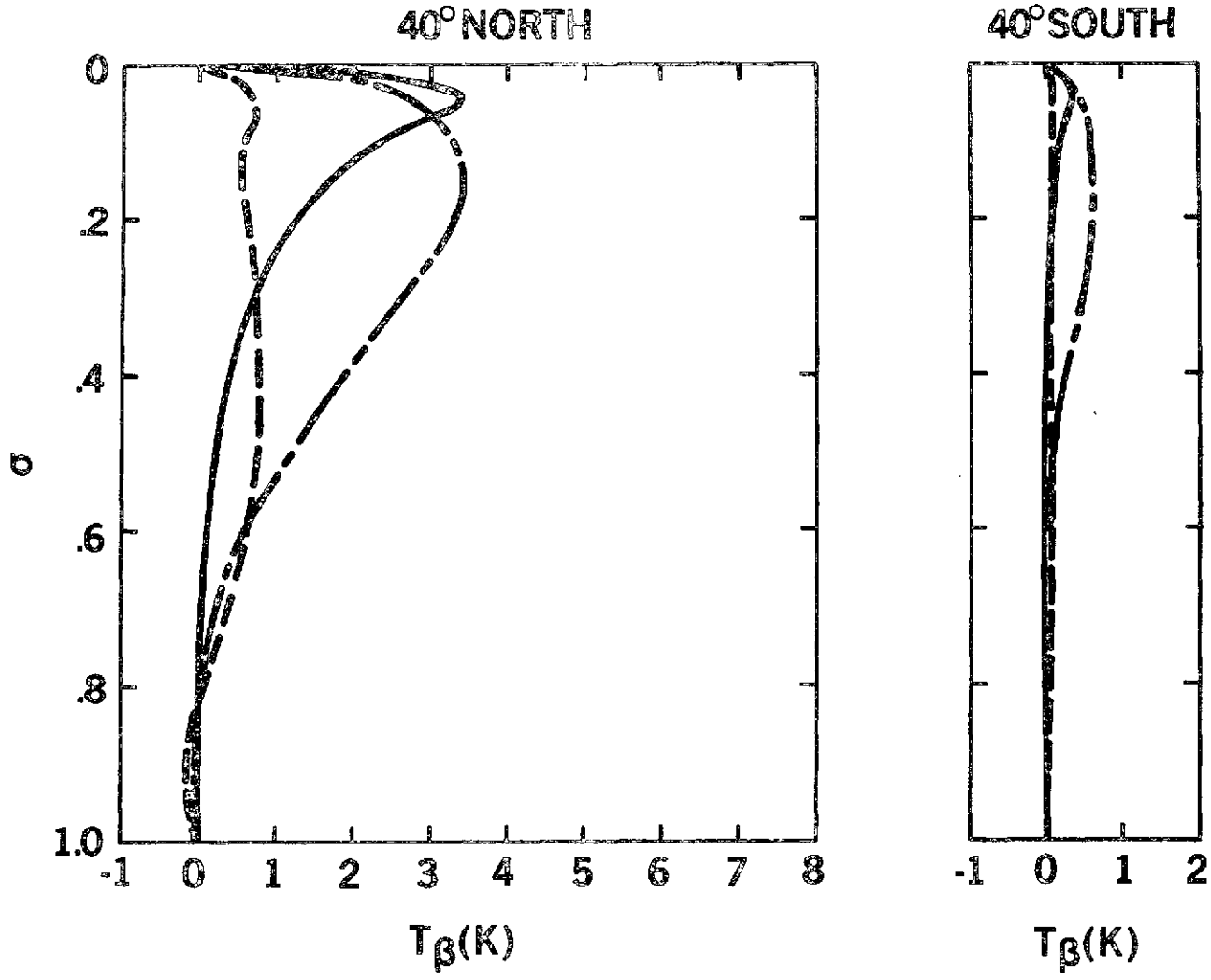

Figure 10. First order temperatures with a one day radiative damping time constant at ±40° latitudes. The solid lines are for $K_M = 10^8 cm^2/sec$, the dot-dashed for 10^7 and the dashed for 10^6.

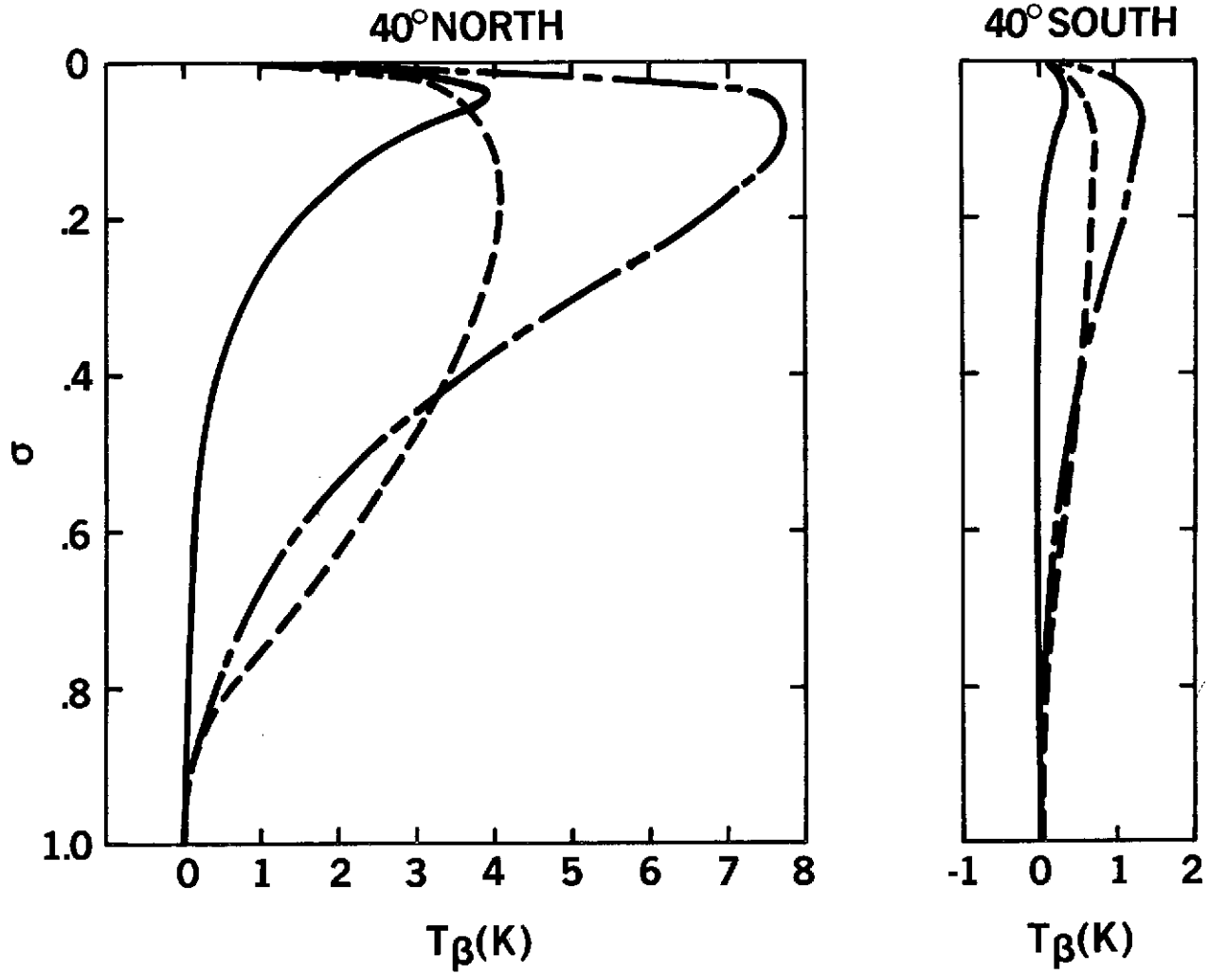

Figure 11. First order temperatures with a ten day radiative damping time constant at ±40° latitudes. The solid lines are for $K_M = 10^8 cm^2/sec$, the dot-dashed for 10^7 and the dashed for 10^6.